Supporting Information

Synergistic Ni–P Co-doping in Pyrite FeS_2 for Efficient Electrocatalytic Nitrate Reduction via a Dissociative Mechanism: A Theoretical Insight

Haitao Sun,[a,#] Jixuan Li,[a,#] Xueshi Song,[a,] Yuwei Yan,[a] Jingxiang Zhao[a,*]*

[a] *Key Laboratory for Photonic and Electronic Bandgap Materials, Ministry of Education, School of Physics and Electronic Engineering, Harbin Normal University, Harbin, 150025, P. R. China*

[*] *To whom correspondence should be addressed. Email: songxueshihsd@163.com (X. Song), zhaojingxiang@hrbnu.edu.cn(J. Zhao).*

[#] *Haitao Sun and Jixuan Li contributed equally to this work.*

Table S1. Comparison of the U_L between our Ni-P/FeS_2 system and the recently reported catalysts.

Catalyst	**U_L (V)**
Ni/Cu (111)	-0.29
Cu@O_v-Cr_2CO_2	-0.36
PdCu/C_7N_6	-0.36
FeN_4	-0.38
Ti/g-CN	-0.39
OsN_4	-0.42
RuN_4	-0.66

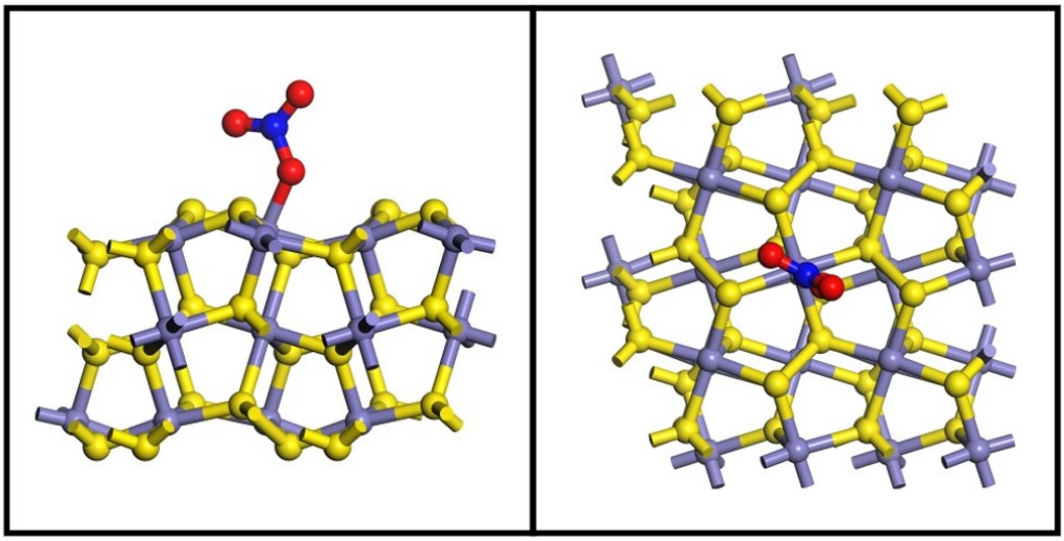

$\Delta G = 0.76eV$

Fig. S1. Optimized adsorption configuration and the associated Gibbs free energy change for NO_3^- on the pristine FeS_2 surface.

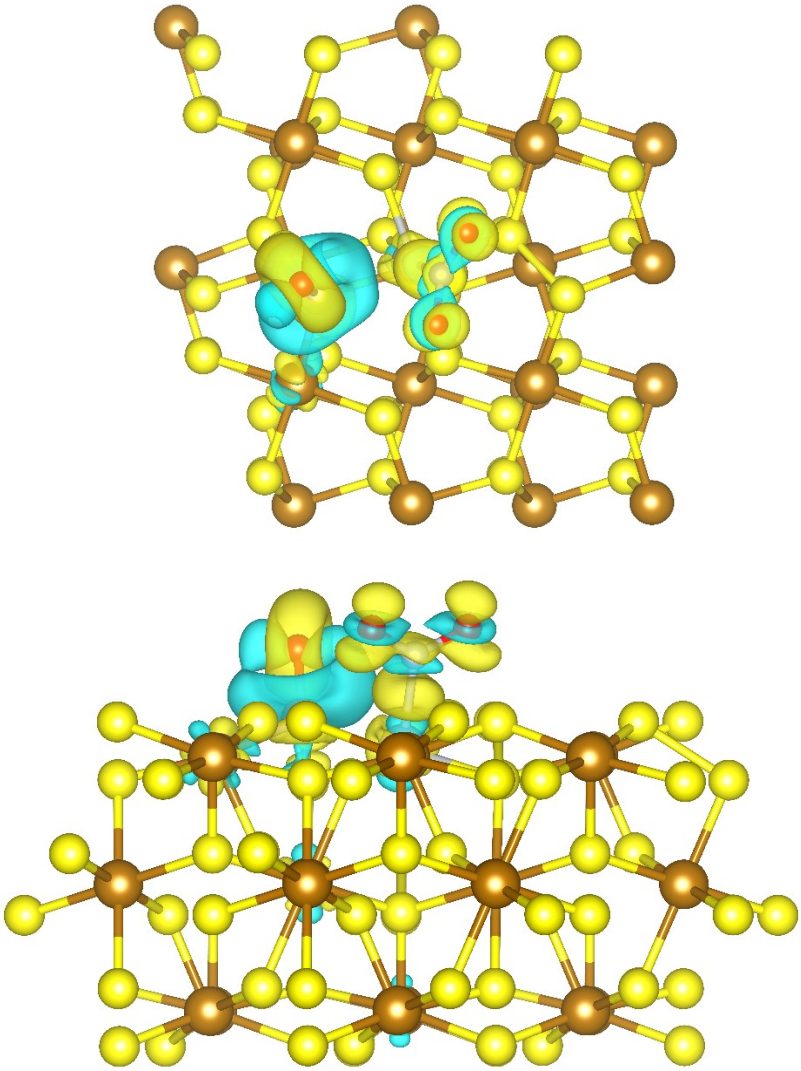

Fig. S2. Differential charge density for the adsorption of NO_3^- species on the Ni-P/FeS_2 catalyst.

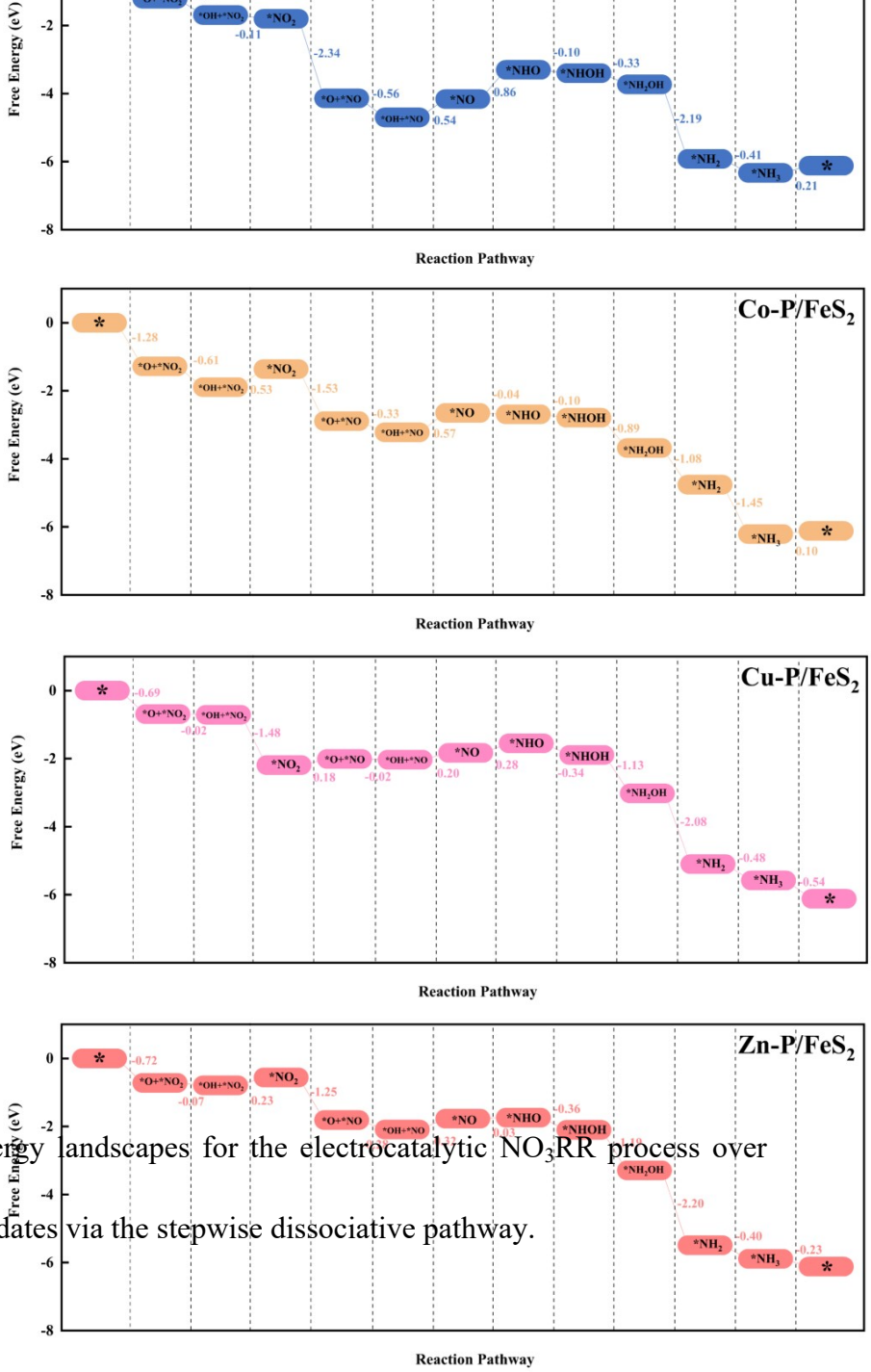

Fig. S3. Gibbs free energy landscapes for the electrocatalytic NO_3RR process over various M-P/FeS_2 candidates via the stepwise dissociative pathway.

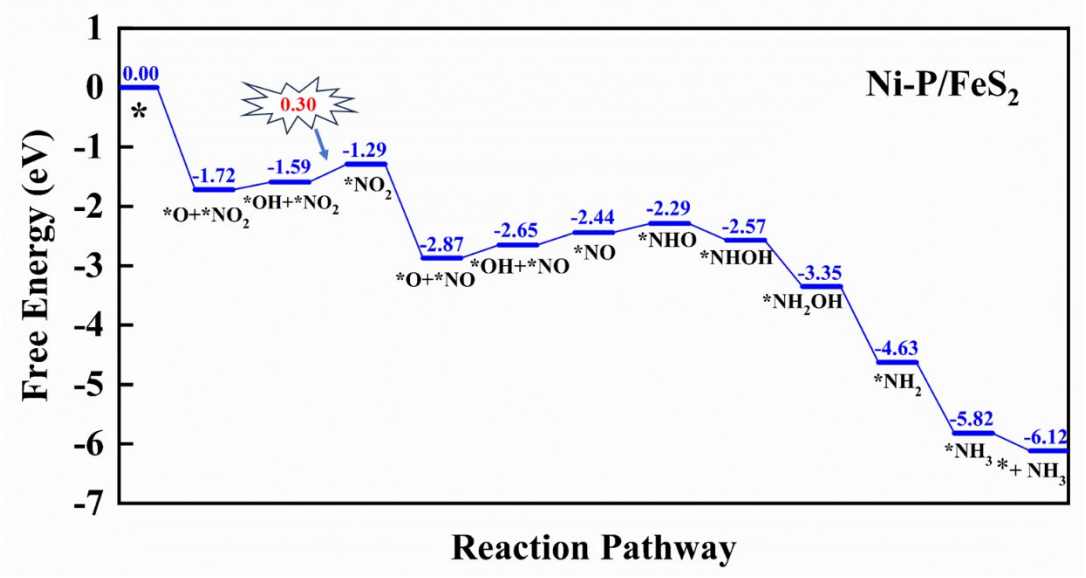

Fig. S4. The computed free energy diagram of NO_3RR on the Ni-P/FeS_2 catalyst by considering the solvent effects using the VASPsol.

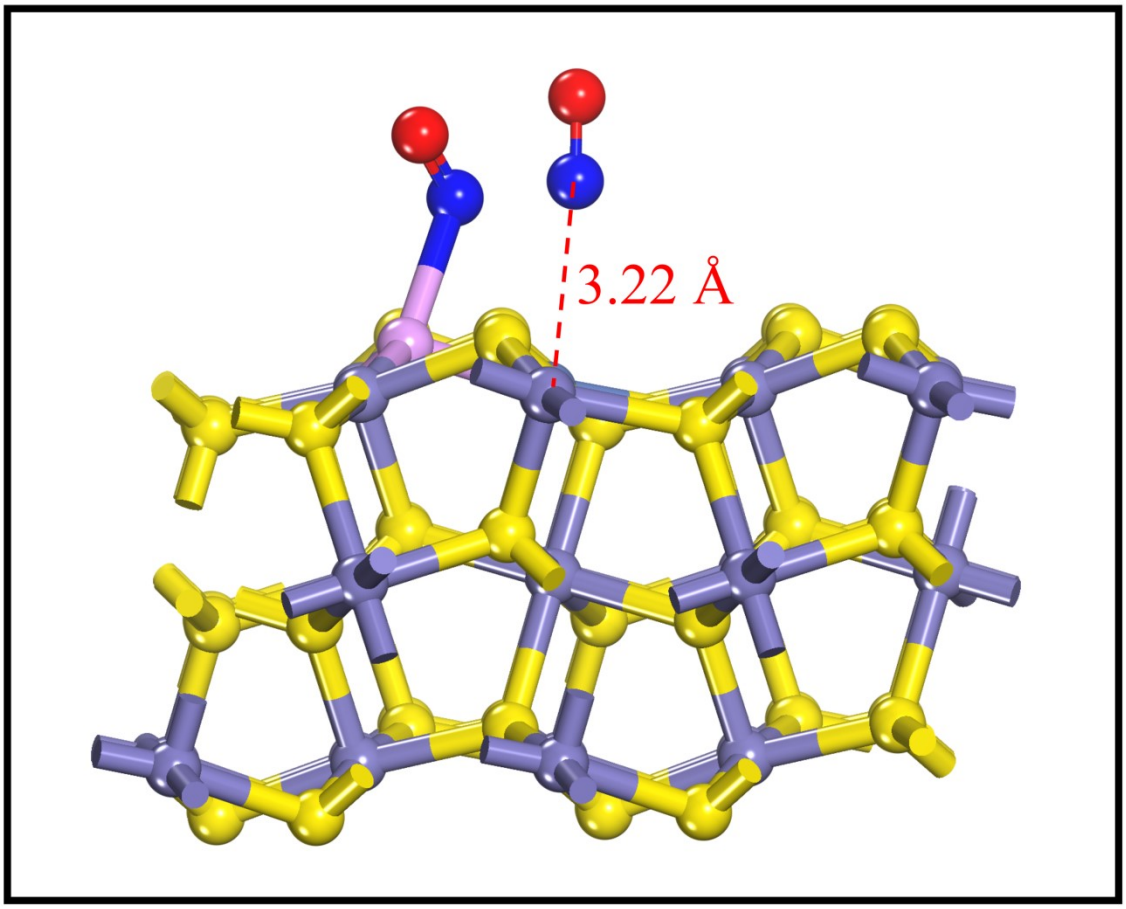

Fig. S5. Optimized adsorption configuration for a secondary NO molecule on the NO^*-preadsorbed Ni-P/FeS_2 catalyst surface.

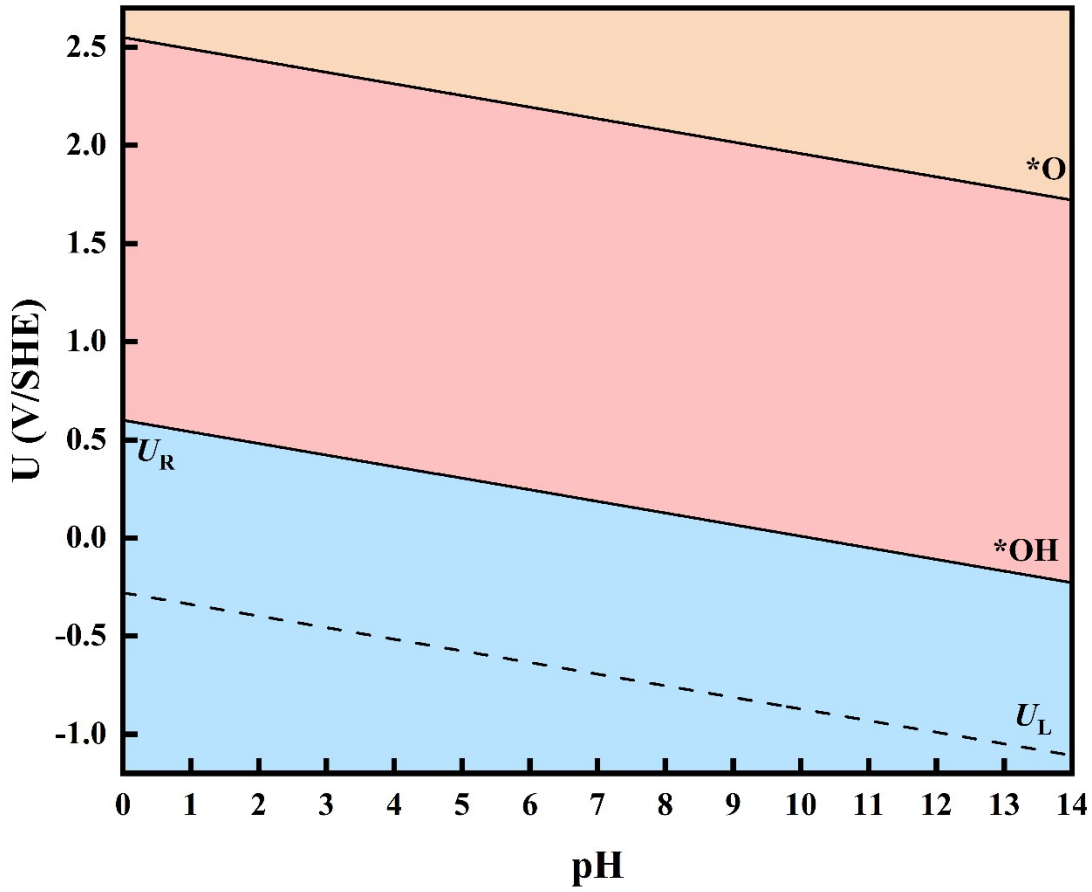

Fig. S6. Pourbaix diagram for the Ni-P/FeS_2 system.